A Common Framework for Inertial Sensor Error Modeling

Juan D. Jurado and John F. Raquet
Air Force Institute of Technology

BIOGRAPHIES

Jan Jurado

Juan Jurado is a doctoral student at the Air Force Institute of Technology. He is an graduate of Texas A&M University, the Air Force Institute of Technology and the Air Force Test Pilot School where he earned B.S.EE, M.S.EE and M.S.FTE degrees, respectively. His previous research includes award-winning papers and projects on ballistic missile search algorithms, electro-optic and Pitot-static calibration techniques, as well as image distortion prediction for navigation sensor fusion. His previous work includes various flight test projects and leadership positions within F-16 and AC-130 flight test squadrons.

John Raquet

John Raquet is the Director of the Autonomy and Navigation Technology (ANT) Center at the Air Force Institute of Technology, where he is also a Professor or Electrical Engineering. He has been involved in navigation research for over 25 years.

ABSTRACT

The availability of an accurate inertial navigation solution depends largely on the proper calibration of the deterministic errors usually found in inertial navigation systems, but more importantly, on the adequate stochastic modeling of the random errors associated with each inertial sensor. As such, a considerable amount of time and energy has been invested in the understanding and modeling of error sources found in a variety of inertial sensor types and their applications. However, a comprehensive review of academic, vendor, and research literature on the subject matter reveals that although the body of knowledge has large depth and breadth, the community lacks consistency across specialty fields with regards to terminology, unit standardization, and modeling techniques.

This paper aims at providing the navigation community with a common framework for the modeling, simulation, and characterization of errors associated with inertial sensor measurements. The goal is not to replace the various inertial error model descriptions that exist, but to provide a common understanding of how these all relate together. After presenting the range of error models and terms found in literature, the subtle differences in terminology and categorization are compared, correlated, and consolidated into a common model. Next, the Allan Variance method is used to carefully and progressively illustrate how each error component in the common model arises and is identified.

The effectiveness of the common model is demonstrated by analyzing stationary data from a real-world inertial measurement unit, comparing the identified error parameters to the vendor specifications, and using the same parameters to produce a simulated signal that closely matches the original. Armed with this common framework, the navigation community will be able to more effectively communicate and exchange ideas on the subject matter, thereby accelerating the progression towards cheaper, more reliable navigation technology with properly modeled inertial sensors at its core.

INTRODUCTION

The availability of an accurate inertial navigation solution depends largely on the proper calibration of the deterministic errors usually found in inertial navigation systems, but more importantly, on the adequate stochastic modeling of the random errors associated with each inertial sensor.

Adequate modeling of inertial sensor errors begins with an understanding of the physical processes from which deterministic and stochastic errors arise. In general, any given sensor output signal can be written in the form

$$\mathbf{y}(t) = \mathbf{M}\mathbf{x}(t) + \varepsilon(t) \tag{1}$$

where $\mathbf{y}(t)$ is the measured output signal, $\mathbf{x}(t)$ is the true signal, $\mathbf{M}$ is a linear operator on $\mathbf{x}(t)$ and $\varepsilon(t)$ is an additive non-linear signal composed of a combination of stochastic and deterministic errors, which vary with sensor type. For inertial sensors, the majority of existing literature adapts a version of (1) to both accelerometers and gyroscopes by providing specific forms of $\mathbf{M}$ and further refining the deterministic components and stochastic processes governing $\varepsilon(t)$.

GENERALIZED ERROR MODEL

In [1] general error models for gyroscopes and accelerometers are provided to describe a wide array of deterministic and stochastic errors. For gyroscopes, [1] describes the relation between true (ω_x) and measured ($\tilde{\omega}_x$) angular rate for a single axis x as

$$\tilde{\omega}_x = (1+S_x)\omega_x + M_y\omega_y + M_z\omega_z + B_{fx} + B_{gx}a_x + B_{gz}a_z + B_{axz}a_xa_z + \eta_x \tag{2}$$

where S_x is the x-axis scale factor, M_y and M_z are cross coupling coefficients, B_{fx} is a constant x-axis bias (non g-sensitive), B_{gx} and B_{gz} are g-sensitive bias coefficients along the input and spin axes, B_{axz} is the anisoelastic bias coefficient, and η_x is zero-mean additive white Gaussian noise. The expanded form in (2) can be applied to the remaining two axes and expressed in terms of (1) by letting

$$\mathbf{y} = \begin{bmatrix} \tilde{\omega}_x \\ \tilde{\omega}_y \\ \tilde{\omega}_z \end{bmatrix} \qquad \mathbf{x} = \begin{bmatrix} \omega_x \\ \omega_y \\ \omega_z \end{bmatrix}$$

$$\mathbf{M} = \begin{bmatrix} 1+S_x & M_y & M_z \\ M_x & 1+S_y & M_z \\ M_x & M_y & 1+S_z \end{bmatrix}$$

$$\varepsilon = \begin{bmatrix} B_{fx} + B_{gx}a_x + B_{gz}a_z + B_{gxz}a_{xz} + \eta_x \\ B_{fy} + B_{gy}a_y + B_{gx}a_x + B_{gyx}a_{yx} + \eta_y \\ B_{fz} + B_{gz}a_z + B_{gy}a_y + B_{gzy}a_{zy} + \eta_z \end{bmatrix}$$

Similarly, [1] also describes a general error model for accelerometers in terms of the relation between true (a_x) and measured ($\tilde{a}_x$) acceleration for a single axis x as

$$\tilde{a}_x = (1+S_x)a_x + M_ya_y + M_za_z + B_f + B_va_xa_y + \eta_x \tag{3}$$

where S_x is the x-axis scale factor, M_y and M_z are cross coupling coefficients, B_f is a constant measurement bias, B_v is the vibro-pendulus error coefficient, and η_x is zero-mean additive white Gaussian noise. Again, (3) can be expressed using the form in (1) by letting

$$\mathbf{y} = \begin{bmatrix} \tilde{a}_x \\ \tilde{a}_y \\ \tilde{a}_z \end{bmatrix} \qquad \mathbf{x} = \begin{bmatrix} a_x \\ a_y \\ a_z \end{bmatrix}$$

$$\mathbf{M} = \begin{bmatrix} 1+S_x & M_y & M_z \\ M_x & 1+S_y & M_z \\ M_x & M_y & 1+S_z \end{bmatrix}$$

$$\varepsilon = \begin{bmatrix} B_f + B_va_xa_y + \eta_x \\ B_f + B_va_ya_z + \eta_y \\ B_f + B_va_za_y + \eta_z \end{bmatrix}$$

Table 1: Allan Variance Noise Parameter Identification Summary

Error Source	Symbol	Relation to Allan Deviation	Tangent Line		Units*
			Slope	τ at desired σ	
Quantization	σ_q	$\sigma(\tau) = \sigma_q\sqrt{3}\tau^{-1}$ $\sigma_q = \frac{\tau\sigma(\tau)}{\sqrt{3}}$	-1	$\sqrt{3}$	[deg] or [m/s]
Random Walk	σ_{rw}	$\sigma(\tau) = \sigma_{rw}\tau^{-1/2}$ $\sigma_{rw} = \tau^{1/2}\sigma(\tau)$	$-1/2$	1	[deg/$\sqrt{\text{hr}}$] or [m/s/$\sqrt{\text{hr}}$]
Bias Instability	σ_b	$\sigma(\tau) = \sigma_b\sqrt{\frac{2\ln 2}{\pi}}\tau^0$ $\sigma_b = \frac{\sigma(\tau)}{\sqrt{\frac{2\ln 2}{\pi}}}$	0	N/A	[deg/hr] or [m/s/hr]
Rate Random Walk	σ_{rrw}	$\sigma(\tau) = \sigma_{rrw}\frac{\tau^{1/2}}{\sqrt{3}}$ $\sigma_{rrw} = \sigma(\tau)\sqrt{3}\tau^{-1/2}$	$1/2$	3	[deg/hr/$\sqrt{\text{hr}}$] or [m/s/hr/$\sqrt{\text{hr}}$]
Rate Ramp	σ_{rr}	$\sigma(\tau) = \sigma_{rr}\frac{\tau^1}{\sqrt{2}}$ $\sigma_{rr} = \sigma(\tau)\sqrt{2}\tau^{-1}$	1	$\sqrt{2}$	[deg/hr/hr] or [m/s/hr/hr]
*Units result from $\sigma(\tau)$ measured in [deg/hr] or [m/s/hr] and τ measured in [hrs]					

Further literature review reveals small differences in name and convention given to the general set of parameters found in gyroscope and accelerometer models. Additionally, the technology used in sensor development (i.e. mechanical, ring laser, MEMS, etc...) affects the combination of parameters found in particular models. In general, however, all models can be expressed as an adaptation of (1), with $\mathbf{M}$ composed of generally deterministic terms and ε composed of a combination of deterministic and stochastic terms. This general distinction between $\mathbf{M}$ and ε found in most literature then allows the discussion to focus not on the number or combination of terms found in a particular model, but on the subtle differences in naming convention and modeling technique for the stochastic terms found in ε.

Focusing on stochastic terms, [2] uses a form similar to (1) and describes three types of stochastic gyroscopic errors in ε as:"constant bias, uncorrelated white noise, and $1/f$ (flicker) noise." Similar terms appear in [3] and [4] as general noise parameters that can be identified using the Allan variance method ([5],[6]), which will be discussed in later sections. Additionally, terms such as "quantization noise", "angle/velocity random walk", "bias instability", "bias stability", "rate random walk" and "rate ramp" appear throughout literature as members of a general group of noise parameters that can be found in various types of inertial sensors. It is important to note that most of these terms are actually variations of an attempt to characterize the stochastic component of ε. That is, out of the eclectic characterization of inertial error terms discussed so far, the majority of the variation in terminology and modeling lies not within $\mathbf{M}$ but actually within ε. This is somewhat logical since, as previously discussed, $\mathbf{M}$ is a linear operator that is mostly consistent across the varying sensor technologies, leaving ε as a stochastic modeling challenge due to differing interpretations across application communities.

As such, the focus of this research now shifts to providing a common framework for the most commonly found terms in ε as well as demonstrating through practical application (via provided code and algorithms in [7]) the identification, modeling and simulation of such noise parameters using real and simulated data.

IDENTIFYING NOISE PARAMETERS

Focusing on identifying the components of ε in a given inertial sensor signal, we begin by reviewing the Allan variance method and how it can be used to characterize stochastic process coefficients for a variety of error sources. Table 1 summarizes the key identification parameters while the published code in [7] provides a sample applied algorithm for MATLAB.

Allan Variance Method

As previously alluded to, although the Allan Variance method was originally developed for analyzing clock performance [8], it has also been proven to be a valuable noise identification tool for inertial sensors ([5],[4],[3],[6]). In general, this method computes a variance, $\sigma^2(\tau)$, and indirectly a deviation, $\sigma(\tau)$, for a given input *rate* signal, $\dot{\mathbf{y}}(t)$, a function of averaging time

(τ) using

$$\bar{\Omega}_k(\tau) = \frac{1}{\tau}\int_{t_k}^{t_k+\tau} \dot{y}(t)dt \qquad \text{[deg/s] or [m/s/s]} \tag{4}$$

$$\sigma^2(\tau) = \frac{1}{2(N-2n)}\sum_{k=1}^{N-2n}[\bar{\Omega}_{t_k+\tau}(\tau) - \bar{\Omega}_k(\tau)]^2 \qquad \text{[deg}^2\text{/s}^2\text{] or [m}^2\text{/s}^2\text{/s}^2\text{]} \tag{5}$$

where $\dot{y}(t)$ is either an angular rate [deg/s] for gyroscopes or a specific force [m/s/s] for accelerometers. We note here one of the first major sources of variation in literature: measurement units. For the purposes of standardization and compatibility with most manufacturer specifications for inertial sensors, the units used throughout this research will not only be clearly laid out for each noise component but also summarized in Table 1. Additionally, it is important to note the basic measurement unit for gyroscopes is established as [deg] while the same unit for accelerometers is established as [m/s]. When referring to each type of sensor's output rate, we simply divide by [s] to produce [deg/s] or [m/s/s], respectively. In the case where an inertial sensor provides measurements in increments ($\Delta\theta$ [deg] or ΔV [m/s]), the corresponding rate signal needed for the Allan variance method can be computed using

$$\dot{y} \approxeq \frac{\Delta y}{\Delta t} \qquad \text{[deg/s]}$$

where Δt is the corresponding sampling period of the inertial sensor. The method by which the Allan variance method produces $\sigma(\tau)$ allows for practical identification of the various components of ε found in an output signal $\mathbf{y}$ by analyzing the logarithmic relationship between $\sigma(\tau)$ and τ. The following sections then focus on the identification of the most commonly found stochastic terms in literature, all of which compose ε in our generalized error model.

Quantization Noise

Quantization noise is the error that arises from the sampling of a continuous signal at discrete steps of size Δ [3]. Quantization noise is uniformly distributed between $-\Delta/2$ and $\Delta/2$, which gives

$$\mu_q = 0 \tag{6}$$

$$\sigma_q^2 = \frac{\Delta^2}{12} \tag{7}$$

$$\sigma_q = \frac{\Delta}{\sqrt{12}} \tag{8}$$

Analyzing the relationship between the power spectral density function and the Allan deviation of a signal composed only of quantization noise [4] gives

$$\sigma(\tau) = \frac{\sigma_q\sqrt{3}}{\tau} = \sigma_q\sqrt{3}\tau^{-1} \qquad \text{[deg/s] or [m/s/s]} \tag{9}$$

$$\sigma_q = \frac{\tau\sigma(\tau)}{\sqrt{3}} \qquad \text{[deg] or [m/s]} \tag{10}$$

$$\log(\sigma(\tau)) = \log(\sigma_q\sqrt{3}\tau^{-1}) \tag{11}$$

$$= -\log(\tau) + \log(\sigma_q) + \log(\sqrt{3}) \tag{12}$$

which tells us we can identify σ_q in an Allan deviation curve by finding a -1 slope when plotting $\log(\sigma(\tau))$ against $\log(\tau)$. Next, letting $\tau = \sqrt{3}$ in (12) solves the equation for σ_q, which means if the -1 slope line is projected to $\tau = \sqrt{3}$, the value of $\sigma(\tau)$ at that point will equal σ_q. This process is illustrated in Figure 3. Finally, (10) tells us the units of σ_q are in [deg] or [m/s] since $\sigma(\tau)$ is assumed to be in [deg/s] or [m/s/s] and τ is in [s]. As summarized in Table 1, the quantization noise coefficient can be identified in an Allan deviation curve by finding a -1 slope when plotting $\log(\sigma(\tau))$ against $\log(\tau)$ and projecting a line with that slope out to $\tau = \sqrt{3}$. The resulting value of $\sigma(\tau)$ as that point will then describe σ_q in [deg] or [m/s].

Angle/Velocity Random Walk

As made clear by the name, angle or velocity random walk is a random walk observed in the angle [deg] or velocity [m/s] signal output of an inertial sensor. In terms of (2) or (3), angle/velocity random walk arises from integrating η_x in $\tilde{\omega}_x$ or $\tilde{a}_x$. The relationship between the Allan deviation and the power spectral density for a signal of this type is given by

$$\sigma(\tau) = \frac{\sigma_{rw}}{\sqrt{\tau}} = \sigma_{rw}\tau^{-1/2} \qquad \text{[deg/s] or [m/s/s]} \tag{13}$$

$$\sigma_{rw} = \tau^{1/2}\sigma(\tau) \qquad \text{[deg/}\sqrt{\text{s}}\text{] or [m/s/}\sqrt{\text{s}}\text{]} \tag{14}$$

$$\log(\sigma(\tau)) = \log(\sigma_{rw}\tau^{-1/2}) \tag{15}$$

$$= -\frac{1}{2}\log(\tau) + \log(\sigma_{rw}) \tag{16}$$

which tells us we can identify σ_{rw} in an Allan deviation curve by finding a $-1/2$ slope when plotting $\log(\sigma(\tau))$ against $\log(\tau)$. Letting $\tau = 1$ in (16) solves the equation for σ_{rw}, which means if the $-1/2$ slope line is projected to $\tau = 1$, the value of $\sigma(\tau)$ at that point will equal σ_{rw}. Equation (14) tells us the units of σ_{rw} are in [deg/$\sqrt{\text{s}}$] or [m/s/$\sqrt{\text{s}}$]. Since in this case the time units were not cancelled out in (14), it becomes important to note that if σ_{rw} is desired in units more compatible with manufacturer specifications (such as [deg/$\sqrt{\text{hr}}$] or [m/s/$\sqrt{\text{hr}}$]), we can either pre-multiply $\sigma(\tau)$ by 3600 [s/hr] and τ by $1/3600$ [hr/s] prior to analyzing the log-log slope, or simply project the line out to $\tau = 3600$ [s] instead of $\tau = 1$ [s].

Bias Instability

Bias instability, sometimes referred to ironically as bias stability, refers to the tendency of an inertial sensor's constant bias (B_f in (2) or (3)) to change or drift during use. The most accurate description of the stochastic process behind this drift is flicker (or $1/f$) noise as shown by [2] and defined in (30). However, due to complications in the modeling of flicker noise in common navigation estimation algorithms (such as a a Kalman filter), this process is often approximated by a first-order Gauss-Markov (FOGM) process. As such, the relation between flicker noise and Allan deviation will be studied for noise identification purposes while the relation between FOGM and Allan deviation will be studied for noise simulation purposes. The relationship between the Allan deviation and the power spectral density for a flicker noise signal is given by

$$\sigma(\tau) = \sigma_b\sqrt{\frac{2\ln 2}{\pi}} = \sigma_b\sqrt{\frac{2\ln 2}{\pi}}\tau^0 \qquad \text{[deg/s] or [m/s/s]} \tag{17}$$

$$\sigma_b = \frac{\sigma(\tau)}{\sqrt{\frac{2\ln 2}{\pi}}} \qquad \text{[deg/s] or [m/s/s]} \tag{18}$$

$$\log(\sigma(\tau)) = 0\log(\tau) + \log(\sigma_b) + \log\left(\sqrt{\frac{2\ln 2}{\pi}}\right) \tag{19}$$

which tells us there is no linear relation to τ in (19). That is, we can identify the flicker noise coefficient in an Allan deviation curve by finding a 0 slope when plotting $\log(\sigma(\tau))$ against $\log(\tau)$. Additionally, (18) tells us the value of $\sigma(\tau)$ at that point can be divided by $\sqrt{\frac{2\ln 2}{\pi}}$ to solve for σ_b, which will be in [deg/s] or [m/s/s]. As previously discussed, if σ_b is desired in units more compatible with manufacturer specifications (such as [deg/hr] or [m/s/hr]), we can pre-multiply $\sigma(\tau)$ by 3600 [s/hr] and τ by $1/3600$ [hr/s] prior to analyzing the log-log slope.

Next, for noise simulation purposes, it is also important to discuss the relationship between the Allan deviation curve and the power spectral density of a FOGM process. This relation is also found in [3] and given by

$$\sigma(\tau) = \sqrt{\frac{(q_c T_c)^2}{\tau}\left[1 - \frac{T_c}{2\tau}\left(3 - 4e^{-\frac{\tau}{T_c}} + e^{-\frac{2\tau}{T_c}}\right)\right]} \tag{20}$$

where T_c is the correlation time and q_c is the noise amplitude. As shown in [3] and [4], (20) can be shown to approach a 0 log-log slope when

$$\tau = 1.89T_c \tag{21}$$

$$\sigma(\tau) = 0.437q_c\sqrt{T_c} \tag{22}$$

That is, if T_c and q_c are correctly chosen, one can approximate the 0 slope Allan deviation curve of flicker noise at the same τ found in the original flicker noise signal. This process will be discussed in more detail in the following sections.

Rate Random Walk

In contrast to angle/velocity random walk, rate random walk refers to a random walk process observed in the inertial sensor's rate signal ([deg/s] or [m/s/s]). In terms of (2) or (3), rate random walk arises from integrating white noise found in $\dot{\tilde{\omega}}_x$ or $\dot{\tilde{a}}_x$. The relationship between the Allan deviation and the power spectral density for a signal of this type is given by

$$\sigma(\tau) = \sigma_{rrw}\sqrt{\frac{\tau}{3}} = \sigma_{rrw}\frac{\tau^{1/2}}{\sqrt{3}} \qquad \text{[deg/s] or [m/s/s]} \tag{23}$$

$$\sigma_{rrw} = \sigma(\tau)\sqrt{3}\tau^{-1/2} \qquad \text{[deg/s/}\sqrt{\text{s}}\text{] or [m/s/s/}\sqrt{\text{s}}\text{]} \tag{24}$$

$$\log(\sigma(\tau)) = \frac{1}{2}\log(\tau) + \log(\sigma_{rrw}) - \frac{1}{2}\log(3) \tag{25}$$

which tells us we can identify σ_{rrw} in an Allan deviation curve by finding a $+1/2$ slope when plotting $\log(\sigma(\tau))$ against $\log(\tau)$. Letting $\tau = 3$ in (25) solves the equation for σ_{rrw}, which means if the $+1/2$ slope line is projected to $\tau = 3$, the value of $\sigma(\tau)$ at that point will equal σ_{rrw}. Equation (24) tells us the units of σ_{rrw} are in [deg/s/$\sqrt{\text{s}}$] or [m/s/s/$\sqrt{\text{s}}$]. If σ_{rrw} is desired in units more compatible with manufacturer specifications (such as [deg/hr/$\sqrt{\text{hr}}$] or [m/s/hr/$\sqrt{\text{hr}}$]), we can either pre-multiply $\sigma(\tau)$ by 3600 [s/hr] and τ by $1/3600$ [hr/s] prior to analyzing the log-log slope, or simply project the line out to $\tau = 10,800$ [s] instead of $\tau = 3$ [s].

Rate Ramp

Finally, rate ramp refers to the deterministic, linear and usually long-term increase of the inertial sensor's rate signal output ([deg/s] or [m/s/s]). In terms of (2) or (3), rate random walk arises when B_{fx} or B_f linearly changes over time with a deterministic slope. The relationship between the Allan deviation and the power spectral density for a signal of this type is given by

$$\sigma(\tau) = \sigma_{rr}\frac{\tau^{1}}{\sqrt{2}} \qquad \text{[deg/s] or [m/s/s]} \tag{26}$$

$$\sigma_{rr} = \sigma(\tau)\sqrt{2}\tau^{-1} \qquad \text{[deg/s/s] or [m/s/s/s]} \tag{27}$$

$$\log(\sigma(\tau)) = \log(\tau) + \log(\sigma_{rr}) - \log(\sqrt{2}) \tag{28}$$

which tells us we can identify σ_{rr} in an Allan deviation curve by finding a $+1$ slope when plotting $\log(\sigma(\tau))$ against $\log(\tau)$. Letting $\tau = \sqrt{2}$ in (28) solves the equation for σ_{rr}, which means if the $+1$ slope line is projected to $\tau = \sqrt{2}$, the value of $\sigma(\tau)$ at that point will equal σ_{rr}. Equation (27) tells us the units of σ_{rr} are in [deg/s/s] or [m/s/s/s]. If σ_{rr} is desired in units more compatible with manufacturer specifications (such as [deg/hr/hr] or [m/s/hr/hr]), we can either pre-multiply $\sigma(\tau)$ by 3600 [s/hr] and τ by $1/3600$ [hr/s] prior to analyzing the log-log slope, or simply project the line out to $\tau = 5.0912 \times 10^3$ [s] instead of $\tau = \sqrt{2}$ [s].

SIMULATING ERROR PROCESSES

Having examined the stochastic processes driving ε in our generalized error model, we can now use the information at hand to simulate such processes. As shown in the following sections, unit conversion and accountability will play a key role in properly simulating these processes. To facilitate the simulation of these processes, all simulated signals will be generated in the *rate* domain ([deg/s] or [m/s/s]) since such a signal can be directly analyzed for Allan deviation using (4) and (5). Additionally, all input coefficients with time dependencies will be assumed to be in typical manufacturer specifications ([hrs] instead of [s]). The published code in [7] contains a sample applied algorithm for simulating each type of noise signal discussed below.

Quantization Noise

Given a desired σ_q [deg] or [m/s], a simulated quantization noise signal can be generated by producing a uniform distribution of the form

$$\Delta = \sigma_q \sqrt{12}$$

$$\underset{\in \mathbb{R}^{N+1}}{y(t_k)} \sim \mathscr{U}(-\frac{\Delta}{2}, \frac{\Delta}{2}) \qquad k = 1, \ldots, N+1 \qquad \text{[deg] or [m/s]}$$

$$\underset{\in \mathbb{R}^{N}}{\dot{y}(t_k)} = \frac{y(t_{k+1}) - y(t_k)}{\Delta t} \qquad \text{[deg/s] or [m/s/s]}$$

where N is the number of samples in the rate signal and Δt is the sampling period [s].

Angle/Velocity Random Walk

Recall an angle/velocity random walk is produced when white Gaussian noise found in a *rate* signal is integrated to produce angle or velocity. However, the signal of interest we are seeking to generate *is* a rate signal. As such, given a desired σ_{rw} [deg/$\sqrt{\text{hr}}$] or [m/s/$\sqrt{\text{hr}}$], a simulated angle/velocity random walk signal can be generated by producing a Normal distribution of the form

$$\sigma'_{rw} = \frac{\sigma_{rw}}{60} \frac{1}{\sqrt{\Delta t}} \qquad \text{[deg/s] or [m/s/s]}$$

$$\underset{\in \mathbb{R}^{N}}{\dot{y}(t_k)} \sim \mathscr{N}(0, \sigma'^2_{rw}) \qquad k = 1, \ldots, N \qquad \text{[deg/s] or [m/s/s]}$$

where N is the number of samples in the rate signal and Δt is the sampling period [s].

Bias Instability

As previously discussed, there are two methods available for simulating the stochastic process that drives bias instability. The most accurate description of this process is flicker noise, also referred to as $1/f$ noise or "pink noise." For the purposes for generating simulated data, it is preferable to use a pink noise generator such as the one shown in the published code in [7]. However, when modeling bias instability in a navigation algorithm such as a Kalman filter, the FOGM approximation to this process is more widely used. Here, the two methods are explained for completeness. First, given a desired σ_b [deg/hr] or [m/s/hr], the corresponding σ'_b in [deg/s] or [m/s/s] is found using

$$\sigma'_b = \frac{\sigma_b}{3600} \qquad \text{[deg/s] or [m/s/s]}$$

Next, for a direct flicker noise simulation, an autoregressive pink noise generator such as MATLAB's `dsp.ColoredNoise` function can be used to produce $\dot{y}(t)$ as outlined in [9] using

$$w(t_k) = 1 + \sum_{k=1}^{63} a_k \dot{y}'(t_n - t_k) \tag{29}$$

$$a_k = (k - \frac{1}{2}) \frac{a_{k-1}}{k} \qquad k = 1, \ldots, 63 \tag{30}$$

$$\underset{\in \mathbb{R}^{N}}{\dot{y}(t_k)} = \sigma'_b \dot{y}'(t_k) \qquad \text{[deg/s] or [m/s/s]} \tag{31}$$

where $w(t_k) \sim N(0,1)$ is white Gaussian noise.

Since modeling flicker noise directly proves to be computationally cumbersome as shown in [2], the most widely used

approximation to flicker noise in bias instability modeling is a FOGM. This type of process can be generated using

$$
\begin{aligned}
T_c &= \frac{\tau_0}{1.89} && [\text{s}] \\
Q_d &= \sigma_b'^2(1-e^{-\frac{2\Delta t}{T_c}}) && [\text{deg}^2/\text{s}^2] \text{ or } [\text{m}^2/\text{s}^2/\text{s}^2] \\
\Phi &= e^{-\frac{\Delta t}{T_c}} && \\
\dot{y}(t_0) &= \sqrt{Q_d}w(t_0) && \\
\dot{y}(t_{k+1}) &= \Phi\dot{y}(t_k) + \sqrt{Q_d}w(t_k) \qquad k = 1,\ldots,N-1 && [\text{deg/s}] \text{ or } [\text{m/s/s}]
\end{aligned}
$$

where τ_0 is the location of the zero-slope region in the Allan deviation plot, $w(t_k) \sim N(0,1)$ is white Gaussian noise, Δt is the sampling period, and N is the number of samples in the rate signal. Here is is important to note the value of τ_0 (and hence the value of T_c) can be found by analyzing the Allan deviation plot of a particular inertial sensor's rate output. This value can then be used to generate a FOGM for simulation or used directly in the Φ matrix of a Kalman filter along with Q_d.

Rate Random Walk

Recall a rate random walk is produced when white Gaussian noise found in the *acceleration* signal (in [deg/s^2] or [m/s/s^2]) is integrated to produce a *rate* signal. As such, given a desired σ_{rrw} [deg/hr/$\sqrt{\text{hr}}$] or [m/s/hr/$\sqrt{\text{hr}}$], a simulated rate random walk signal can be generated by producing a Normal distribution of the form

$$
\begin{aligned}
\sigma_{rrw}' &= \frac{\sigma_{rrw}}{3600 \times 60}\frac{\sqrt{\Delta t}}{\Delta t} && [\text{deg/s}^2] \text{ or } [\text{m/s/s}^2] \\
\underset{\in\mathbb{R}^N}{\ddot{y}(t_k)} &\sim \mathcal{N}(0, \sigma_{rrw}'^2) \qquad k = 1,\ldots,N && [\text{deg/s}^2] \text{ or } [\text{m/s/s}^2] \\
\underset{\in\mathbb{R}^N}{\dot{y}(t_k)} &= \sum_{n=1}^{k} \ddot{y}(t_n)\Delta t && [\text{deg/s}] \text{ or } [\text{m/s/s}]
\end{aligned}
$$

where N is the number of samples in the rate signal and Δt is the sampling period [s].

Rate Ramp

Recall a rate ramp is observed when the inertial sensor's rate signal (in [deg/s] or [m/s/s]) changes linearly with time. In other words, the output signal (in [deg] or [m/s]) is accelerating. As such, given a desired σ_{rr} [deg/hr/hr] or [m/s/hr/hr], a simulated rate ramp signal can be generated by integrating a constant acceleration term that is equal to the slope of the desired rate ramp to produce the ramping rate signal using

$$
\begin{aligned}
\underset{\in\mathbb{R}^N}{\ddot{y}(t_k)} &= \sigma_{rr}' = \frac{\sigma_{rrw}}{3600 \times 3600} && [\text{deg/s/s}] \text{ or } [\text{m/s/s/s}] \\
\underset{\in\mathbb{R}^N}{\dot{y}(t_k)} &= \sum_{n=1}^{k} \ddot{y}(t_n)\Delta t && [\text{deg/s}] \text{ or } [\text{m/s/s}]
\end{aligned}
$$

where N is the number of samples in the rate signal and Δt is the sampling period [s].

EXPERIMENTAL RESULTS

The concepts explored in the previous sections where put to practice via two methods:

1. Given desired $\sigma_q, \sigma_{rw}, \sigma_b, \sigma_{rrw}, \sigma rr$ coefficients, generate a simulated rate signal, then analyze via Allan deviation to compare input and output values.

2. Given experimental stationary rate data for an inertial sensor, use Allan deviation to extract noise coefficients, generate simulated data with the coefficients found and compare the resulting Allan deviation curve with the original as well as specifications.

Table 2: Allan Variance Noise Parameter Identification Summary

Error Source	Symbol	True Parameter	Identified Parameter	
			Flicker	FOGM
Quantization	σ_q	2.00×10^{-4}	2.00×10^{-4}	2.00×10^{-4}
Random Walk	σ_{rw}	0.80×10^{-2}	0.99×10^{-2}	1.04×10^{-2}
Bias Instability	σ_b	1.00×10^{-1}	1.62×10^{-1}	1.89×10^{-1}
Rate Random Walk	σ_{rrw}	1.00×10^{0}	1.49×10^{0}	1.63×10^{0}
Rate Ramp	σ_{rr}	5.00×10^{0}	4.70×10^{0}	5.22×10^{0}
*FOGM simulated using $T_c = 22.7$ [s],$\Phi = 1.0, Q_d = 2.72 \times 10^{-13}$[deg^2/s^2]				

Table 3: Sensonor STIM-300 Results

Error Source	Symbol	Specification Parameter	Identified Parameter
Accelerometer			
Velocity Random Walk	σ_{rw}	0.06	0.05
Bias Instability	σ_b	2.66*	2.99
Gyroscope			
Angular Random Walk	σ_{rw}	0.15	0.15
Bias Instability	σ_b	0.50	0.67
* converted from [mg] to [m/s/hr]			

The methods listed in (1) and (2) are demonstrated in the published code in [7]. The results are shown in Figures 1 through 6.

Method (1) was completed by selecting the noise coefficients shown in Table 2 and comparing the input and output values computed via the Allan deviation method. Figure 1 and Figure 4 illustrate direct flicker noise simulation and FOGM approximation for σ_b respectively. Figure 2 illustrates the underlying slope detection algorithm for Allan deviation as performed in [7].

Method (2) was completed by collecting 6.057 [hrs] of $\Delta\theta$ and ΔV data at $\Delta t = 0.004$ [s] sampling period from a Sensonor STIM-300 inertial measurement unit. The data was analyzed via the Allan deviation method and the computed noise coefficients were then used to generate simulated data, which was compared to the original data via the Allan deviation method as shown in Figures 5 and 6. Table 3 summarizes the identified noise parameter coefficients and compares their values to those found in the manufacturer specifications [10].

CONCLUSIONS

In summary, this research has demonstrated the use of a generalized inertial sensor error model by consolidating terminology found throughout literature and applying the theoretical concepts to practical algorithms. This paper aimed at providing readers with a centralized source of theory and application for inertial sensor error modeling and simulation by fusing the eclectic source of information available on the subject matter and providing detailed information on the steps necessary to identify and reproduce specific noise coefficients in an inertial sensor rate signal.

DISCLAIMER

The views expressed in this paper are those of the authors, and do not reflect the official policy or position of the United States Air Force, Department of Defense, or U.S. Government.

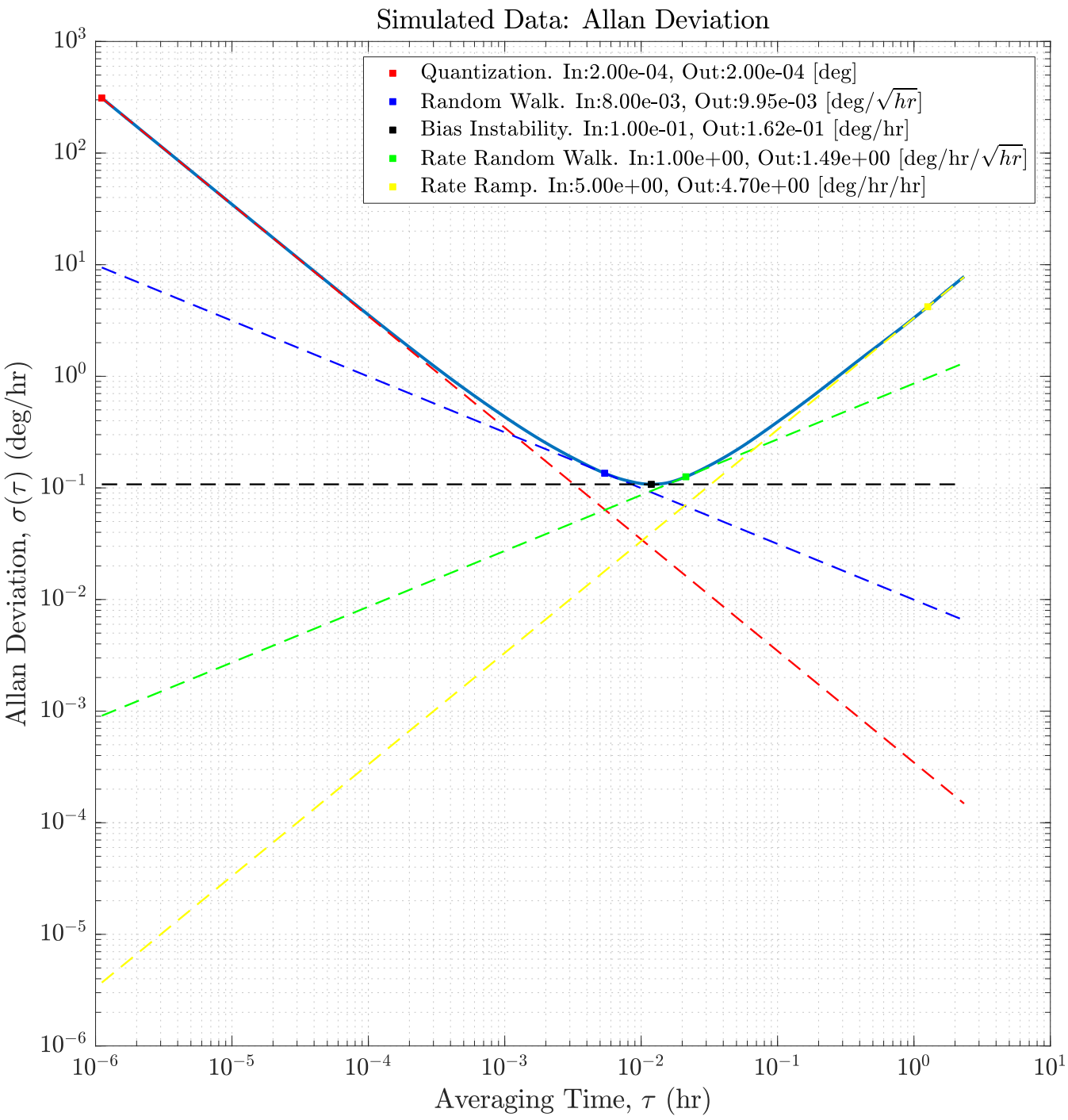

Figure 1: Noise Simulation and Allan Deviation Validation Results

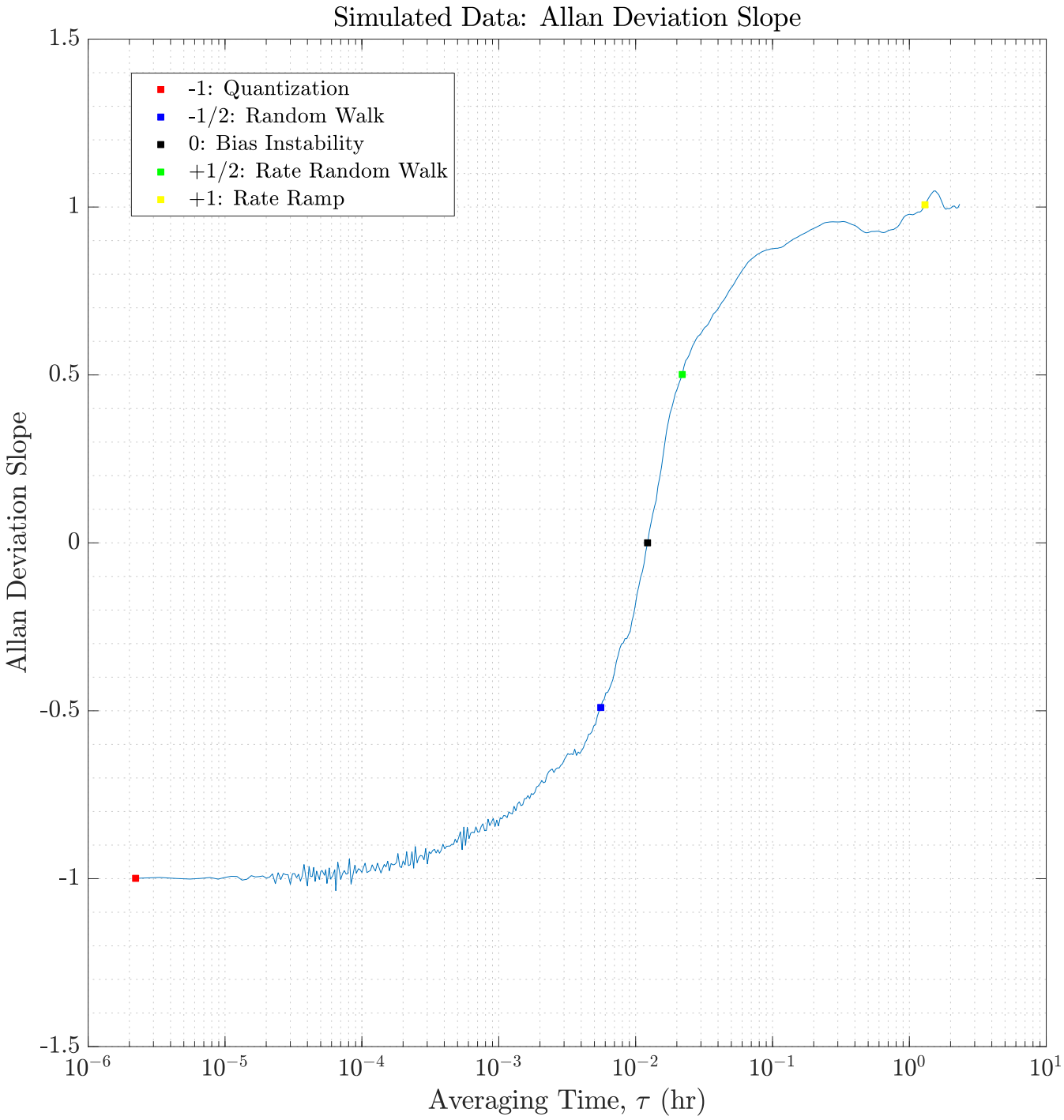

Figure 2: Automated Log-Log Slope Identification Demonstration

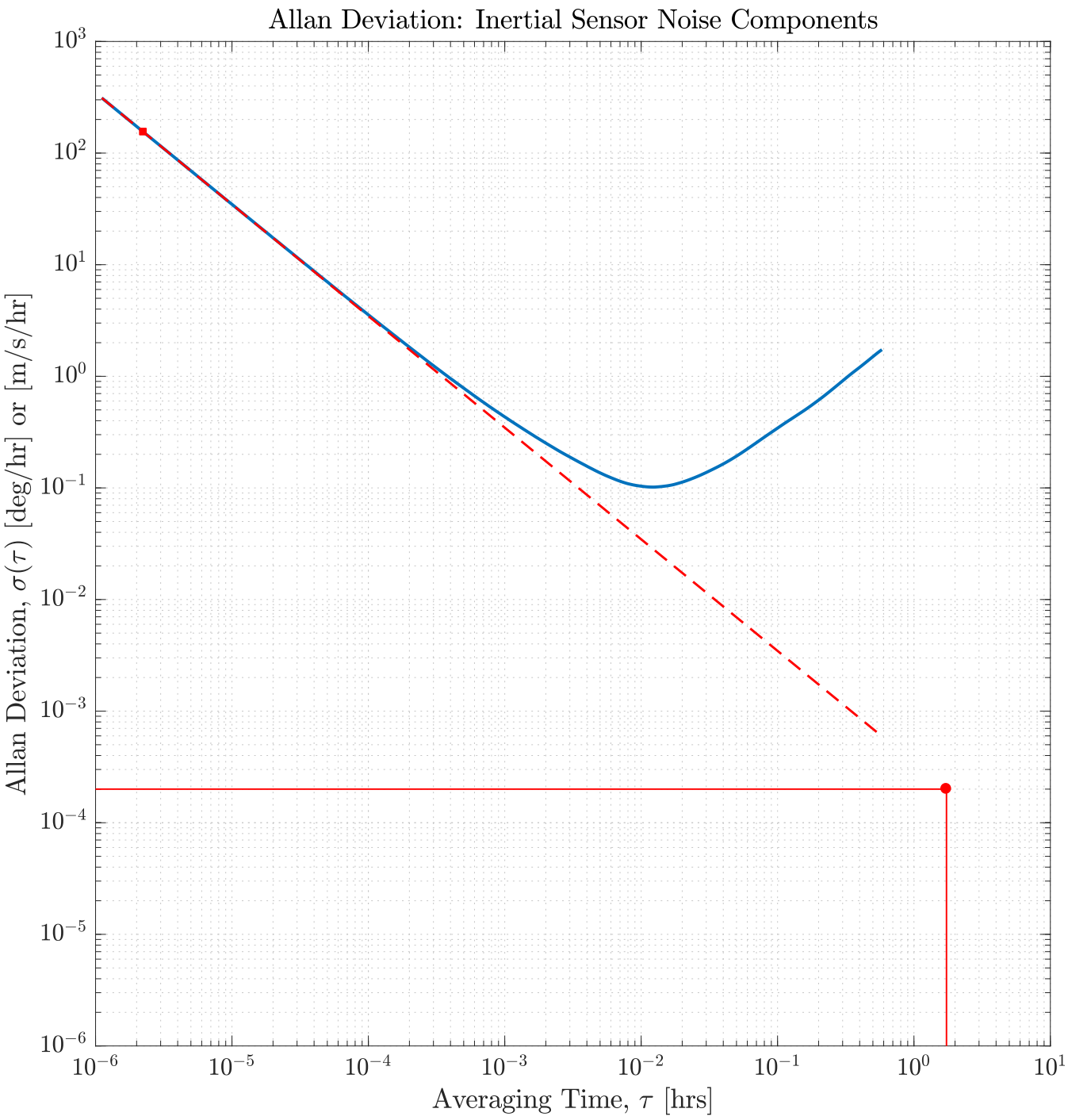

Figure 3: Illustration of Solving for σ_q

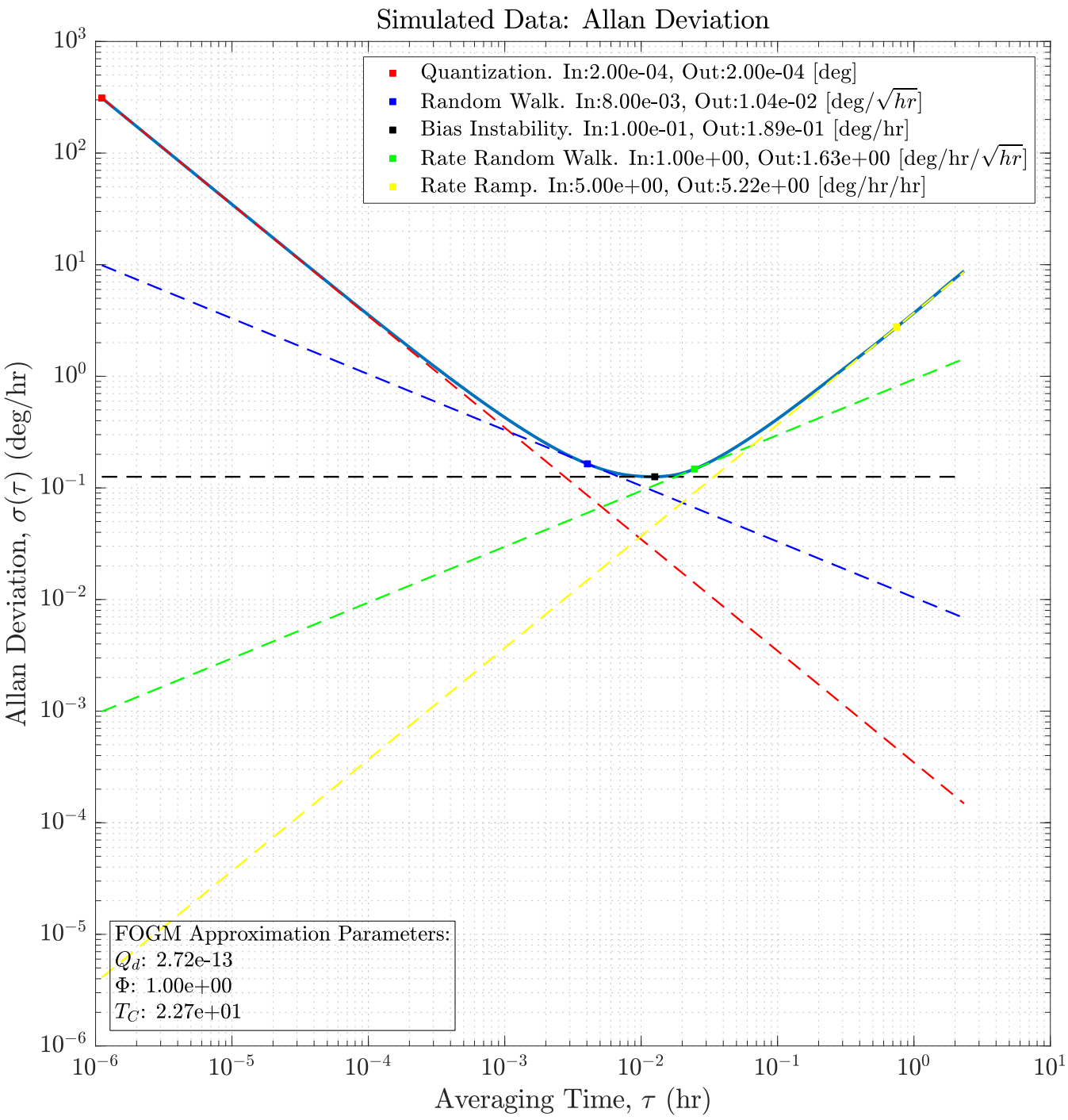

Figure 4: Results of Using FOGM Process to Approximate Flicker Noise

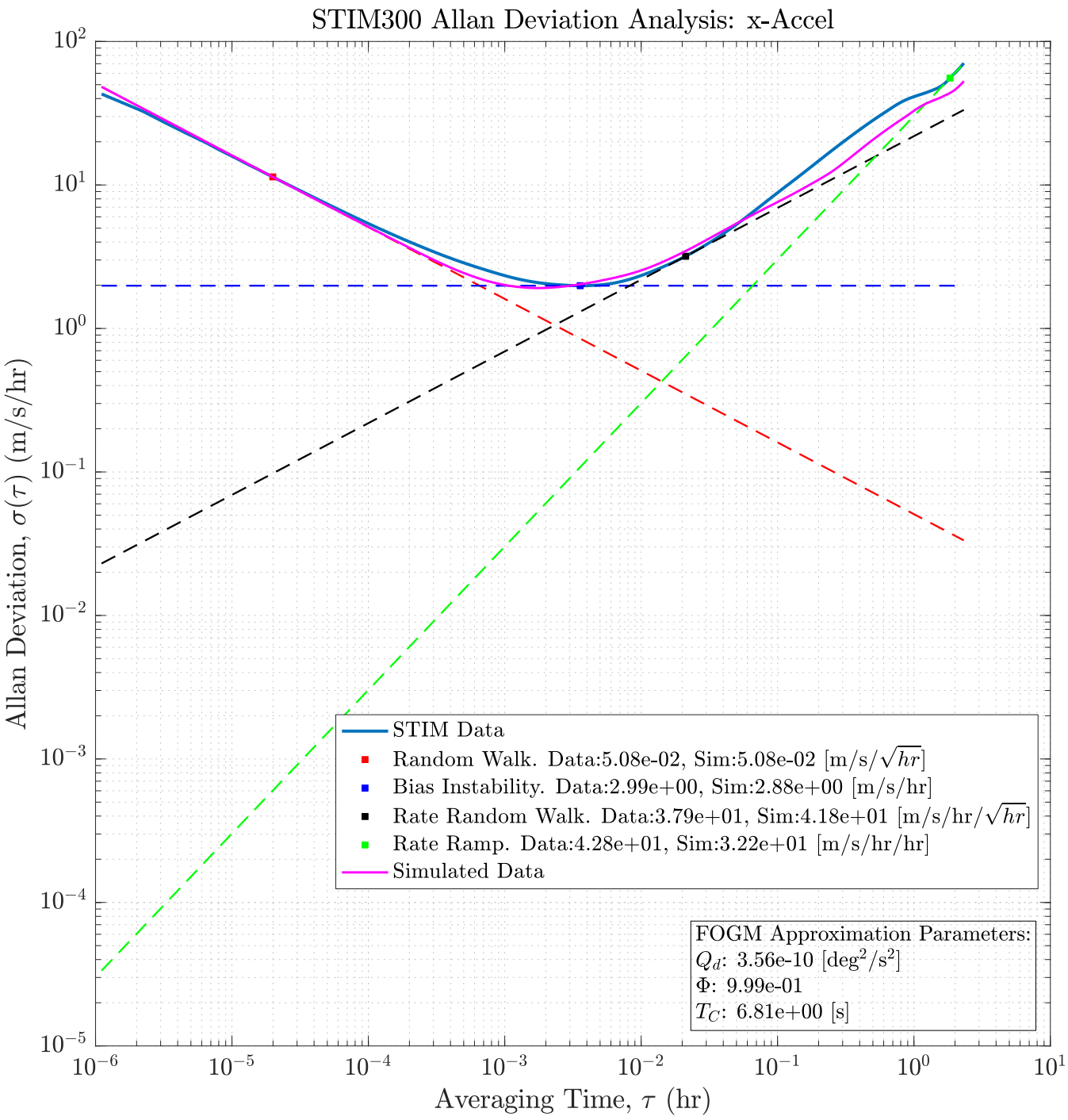

Figure 5: Analysis and Regeneration Results for Sensonor STIM-300 Accel Data

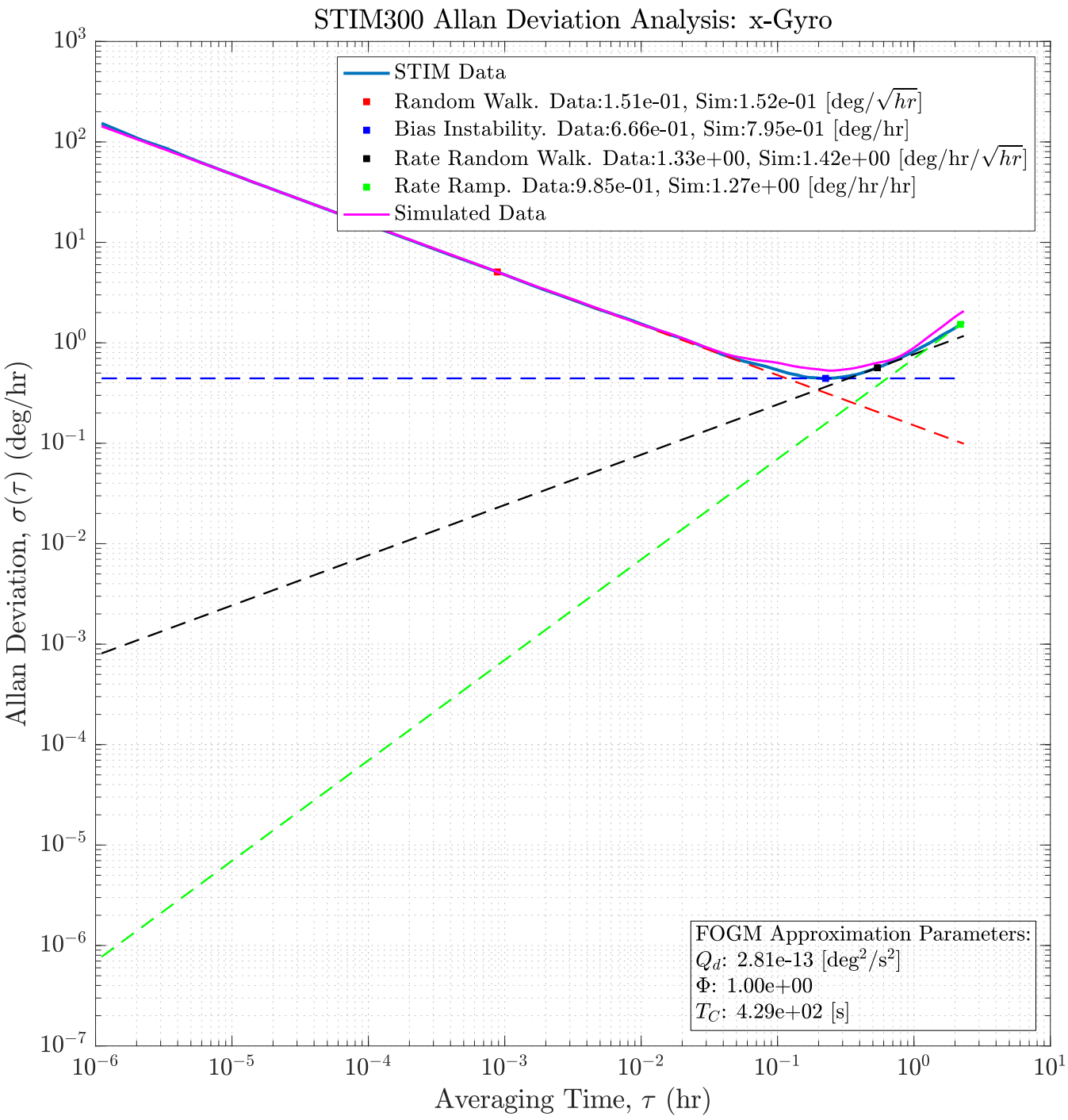

Figure 6: Analysis and Regeneration Results for Sensonor STIM-300 Gyro Data

REFERENCES

[1] D. Titterton and J. Weston, *Strapdown Inertial Navigation Technology, Second Edition*, vol. 207. AIAA, 2005.

[2] M. Kirkko-Jaakkola, J. Collin, and J. Takala, "Bias prediction for MEMS gyroscopes," *IEEE Sensors Journal*, vol. 12, pp. 2157–2163, June 2012.

[3] IEEE, "IEEE standard specification format guide and test procedure for single-axis interferometric fiber optic gyros," *IEEE Std 952-1997*, 1998.

[4] H. Hou, "Modeling inertial sensor errors using allan variance," Master's thesis, University of Calgary, September 2004.

[5] N. El-Sheimy, H. Hou, and X. Niu, "Analysis and modeling of inertial sensors using allan variance," *IEEE Transactions on instrumentation and measurement*, vol. 57, no. 1, pp. 140–149, 2008.

[6] Freescale Semiconductor, Inc., "Allan Variance: Noise Analysis for Gyroscopes." `http://cache.freescale.com/files/sensors/doc/app_note/AN5087.pdf`, 2015.

[7] J. Jurado, "Tools for inertial allan variance analysis and simulation." `https://www.mathworks.com/matlabcentral/fileexchange/61777-tools-for-inertial-allan-variance-analysis-and-simulation`, February 2017.

[8] D. W. Allan, "Statistics of atomic frequency standards," *Proceedings of the IEEE*, vol. 54, pp. 221–230, Feb 1966.

[9] N. J. Kasdin, "Discrete simulation of colored noise and stochastic processes and 1/falpha;power law noise generation," *Proceedings of the IEEE*, vol. 83, pp. 802–827, May 1995.

[10] Sensonor AS, "STIM 300 Inertial Measurement Unit Datasheet." `http://www.sensonor.com/media/91313/ts1524.r8%20datasheet%20stim300.pdf`, April 2013.